Multiphoton ionization spectroscopy of the sodium dimer

John Keller and John Weiner
Department of Chemistry, University of Maryland, College Park, Maryland 20742
(Received 27 June 1983)

We report an investigation of the role of molecular multiphoton ionization in the production of Na_2^+ when sodium vapor is subjected to intense optical radiation. Previous authors attribute the source of *much* of the ion dimer signal to laser-induced associative ionization of atom sodium. In this experiment, we distinguish the molecular process from atomic collisional mechanisms by producing an intense molecular beam created through free-jet expansion of the metal vapor. The beam of nearly 50% dimers cooled to their low rotational and vibrational states allow us to obtain a simplified three-photon ionization spectrum. We find that the spectrum displays two-photon resonances corresponding to known Rydberg level transitions and that the A state, acting as virtual intermediate, plays a crucial role in the large peak-to-peak intensity variations. We employ a simple model of multiphoton ionization which uses a rate-equation approach to generate a calculated spectrum. Based on the experimental results and the success of the model in reflecting them, we conclude that much of the highly structured component of the dimer ion signal reported previously under different experimental conditions is probably due to molecular multiphoton ionization but that this structure rides on a slowly varying broad signal envelope due to laser-induced associative ionization.

INTRODUCTION

When an intense laser beam with wavelengths ranging from 5700 to 6100 Å is directed through sodium vapor, Na_2^+ is formed. Ion dimer spectra were observed by Polak-Dingels *et al.*,[1] using crossed effusive sodium beams, and by Roussel *et al.*,[2] using a cell. They found that the spectra are highly structured. The mechanism by which these dimer ions are produced and the source of this structure have recently become the focus of a great deal of interest,[3,4] and as a result of their investigations, Boulmer and Weiner[3] were able to narrow the list of possible mechanisms to two. They are laser-induced associative ionization,

$$Na+Na+2\hbar\omega \rightarrow Na_2^+ + e^- \quad (1)$$

and multiphoton ionization (MPI) of sodium dimers,

$$Na_2+3\hbar\omega \rightarrow Na_2^+ \ . \quad (2)$$

Boulmer and Weiner showed that much of the Na_2^+ must originate from atomic collisions. First, by direct monitoring of the Na_2 dimers in crossed-beam conditions through photoionization with uv light, they found that Na_2^+ production is not directly proportional to Na_2 density. Second, they observed that when the ground-state atom population is removed, much of the sodium-ion dimer signal is effectively quenched. Third, they showed that the time dependence of ionization follows the laser pulse, thereby eliminating all collisional processes involving real excited states.

However, the narrow peaks (with widths on the order of one wave number), comprising the complicated structure in the spectra, are suggestive of MPI rather than collisional processes. Since laser-induced associative ionization is a free-bound transition in the nuclear wave functions, one would expect that any structure due to modulation of the Franck-Condon overlap would be rather broad compared to what is observed. Boulmer and Weiner suggested rather exotic effects, such as collisional or Feschbach resonances, as possible explanations of the sharp structure. It seems, though, that a simpler, more obvious explanation would be multiphoton ionization of the small amount of dimer contamination in the atomic beam.

On the other hand, the peaks do not appear to match well-known transitions to the sodium A state or the two-photon transitions to known Rydberg levels in this region. Furthermore, the spectrum does not exhibit the features one normally sees in conventional spectroscopy. Instead of the usual band heads and band head progressions, we observe a large number of peaks of seemingly random intensity and position with no apparent relation to the known sodium molecular constants. If the spectral structure is indeed due to multiphoton ionization then, clearly, we need to develop a deeper understanding of this process in Na_2.

We report here the results of a study examining more closely the dimer mechanism. We formed an intense beam of vibrationally and rotationally cooled sodium dimers through free-jet expansion of sodium vapor. By subjecting the beam to an intense laser pulse scanning between 6100 and 5780 Å, we recorded a MPI spectrum of Na_2. The absence of hot bands greatly simplifies the spectrum, allowing us to assign the more intense peaks to two-photon resonances populating the Rydberg level $(3s+5s)^1\Sigma_g^+$, according to the scheme (see Fig. 1)

$$X^1\Sigma_g^+(v'',J'') \rightarrow [A\,^1\Sigma_u^+(v'J')] \rightarrow (3s+5s)^1\Sigma_g^+(v,J) \ , \quad (3)$$

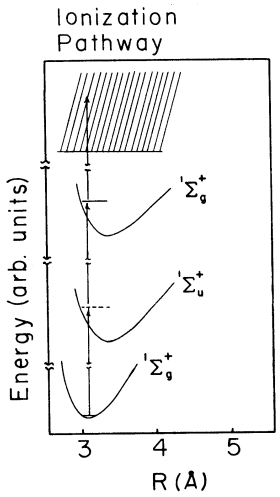

FIG. 1. Na_2 three-photon ionization pathway. The molecule first undergoes two-photon absorption to a Rydberg level which then photoionizes by absorbing a third photon.

where the square brackets denote a virtual intermediate state. We base our assignments on the molecular constants given by Morgan, Xia, and Schawlow (MXS).[5] We find that these constants match quite well the observed spectrum for transitions from the lowest vibrational level ($v''=0$) Na_2 X state to the $v=15$–21 vibrational levels of the Rydberg electronic state. Beyond $v=21$ the match between the calculated and measured band heads becomes progressively less certain. We presume that extrapolating to vibrational levels too far beyond the levels from which the molecular constants were originally derived leads to the observed loss of accuracy. Also of interest, we find that the (14,0) band head is shifted over 3 Å to the blue, indicating a perturbation in the potential curve.

A portion of this spectrum was previously observed by Feldman and reported in her thesis,[6] but no analysis was given since, at the time, little was known of the sodium dimer Rydberg levels.

The relative intensities of the bands can be explained largely on the basis of two features:

(1) the magnitude, $\Delta\omega_i$, of the differences between the energy of the laser photon and the energy of the nearest allowed single-photon transition;

(2) the product of the Franck-Condon factors between the X to A states and the A to Rydberg states.

With a simple model of the dynamics of MPI which incorporates these effects, we are able to calculate a spectrum that reproduces the spectral features of the effusive beam result[1,3] in the region where the spectroscopic constants give accurate values. We conclude that, at least in this restricted region, the highly structured component of the spectrum is due to MPI and not to laser-induced collisions.

EXPERIMENTAL

We modified the experimental apparatus described previously in Ref. 3 to optimize conditions for sodium molecular studies (see Fig. 2). We replaced two crossed effusive sodium beams with a single beam formed by free-jet or supersonic expansion of sodium vapor. The use of a single sodium jet reduces the number of atomic and molecular collisions while providing an intense beam of sodium dimers. In addition, the dimers are cooled to their lower rotational and vibrational states.

The beam is created by a nozzle with a double-oven design. The first oven contains a reservoir of sodium metal which is heated to a temperature that defines the vapor pressure in the nozzle. Free-jet expansion of the vapor, through a 0.5-mm hole in the second oven, forms the beam. To prevent the hole from clogging, we keep the temperature of the second oven at least 50°C above the first. A water-cooled jacket with a 1-cm-diam opening located 1 cm directly in front of the nozzle hole surrounds the source. The jacket acts as a heat shield and helps to collimate the beam as well as to condense excess sodium vapor.

The source is placed inside the vacuum chamber and oriented so that the sodium beam intersects a laser beam at right angles about 10 cm from the nozzle. The point of intersection is located inside the first stage of a two-field time-of-flight mass spectrometer[7] mounted on the vertical axis. The mass spectrometer analyzes atomic and molecular ions formed synchronously with the laser pulses.

For a steady molecular beam intensity we found the optimal oven temperature of the nozzle to be 600°C. At this temperature sodium vapor pressure is near 25 Torr.

The laser is a commercially available Nd^{3+}:YAG-pumped dye laser. It provides an intense source of tunable laser pulses about 13 ns long with a spot diameter of about 1 mm. In these experiments we reduced the laser beam intensity to near 10^6 W cm^{-2}.

By mixing the frequency-doubled dye laser output with the fundamental of the Nd^{3+}:YAG, we produced uv radiation of sufficient energy to directly photoionize both atomic and molecular sodium. From direct measurement of the Na^+ and Na_2^+ signal together with the known cross section of sodium atomic and molecular photoionization[8] we calculated a dimer fraction of 50%. We found

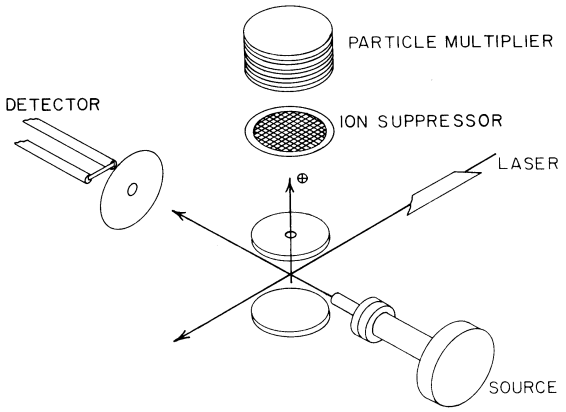

FIG. 2. Schematic of the apparatus. Ions created in the interaction region defined by molecular and laser beam intersection are directed up a time-of-flight tube and detected with a particle multiplier.

no evidence of cluster formation in the sodium beam.

Upon substituting the intense visible laser for the uv beam, we recorded the spectrum of Na_2^+ from 5750 to 6030 Å. A portion of the spectrum, uncorrected for the laser gain curve, is shown in Fig. 3(b). Note the considerable simplification over the effusive beam spectrum shown in Fig. 4(b). We find good agreement with the portion of the spectrum previously observed by Feldman.[6]

THE CALCULATED SPECTRUM

The three-photon ionization spectrum in the spectral range under study is associated with two-photon transitions resonantly enhanced by the $(3s+5s)^1\Sigma_g^+$ Rydberg state, and therefore, the overall three-photon ionization process is resonance enhanced. As illustrated in Fig. 1, the molecule is excited to the Rydberg state through two-photon absorption and is subsequently ionized by absorbing a third photon. An alternate pathway would have the molecule absorb one photon to the A state and then photoionized by absorbing two photons. The observed spectrum does not exhibit ion peaks corresponding to this second pathway indicating that under our experimental conditions it is not important.

We model the production of ions using a rate equation approach.[9,10] The populations of the ground state $N_0(t)$, the Rydberg state $N_1(t)$, and the ions $N_3(t)$ are given by

$$\frac{dN_0(t)}{dt} = -\sigma_1 I^2 N_0(t) , \tag{4a}$$

$$\frac{dN_1(t)}{dt} = \sigma_1 I^2 N_0(t) - (\sigma_2 I + \gamma) N_1(t) , \tag{4b}$$

$$\frac{dN_3(t)}{dt} = \sigma_2 I N_2(t) . \tag{4c}$$

Here, σ_2 is the photoionization cross section. The term γ represents all first-order relaxation losses from the Rydberg level, I represents the laser photon flux, and σ_1 is the two-photon absorption cross section given by

$$\sigma_1 = \frac{8\pi}{2\hbar^2 c^2} \frac{\omega^2}{\Gamma} \left| \sum_i \frac{\mu_{0i}\mu_{i2}}{\Delta\omega_i} \right|^2 , \tag{5}$$

where μ_{lm} are the transition dipole moments coupling the initial and final states through the intermediate states, Γ represents a phenomenological two-photon line width, ω is the laser frequency, and the sum is over the intermediate states.

Generally the sum in Eq. (5) will be dominated by the term with the largest intermediate state coupling, i.e., small $\Delta\omega_i$. However, when more than one intermediate state contributes significantly to the two-photon cross section, interference effects will modulate the size of the cross section. To simplify the calculation, we ignore these interference effects by replacing Eq. (5) with the modified expression

$$\sigma_1 = \frac{8\pi}{2\hbar^2 c^2} \frac{\omega^2}{\Gamma} \sum_i \frac{|\mu_{0i}|^2 |\mu_{i2}|^2}{\Delta\omega_i^2} , \tag{6}$$

where we have removed the cross products in the expansion of the square of the sum.

If we assume a square wave laser pulse of length t, Eqs. (4) are easily integrated to give the ion production,

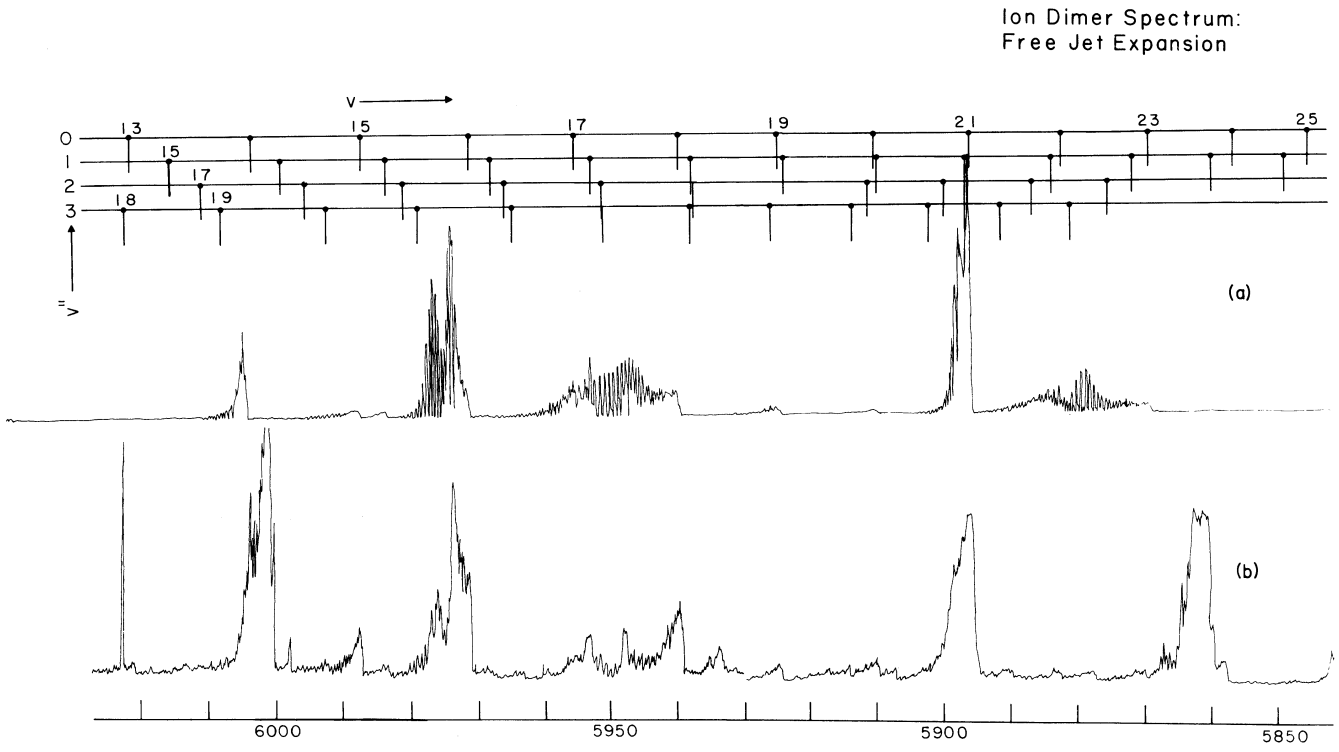

FIG. 3. (a) Model calculation of jet-cooled MPI spectrum of Na_2. (b) Observed MPI spectrum of jet-cooled Na_2.

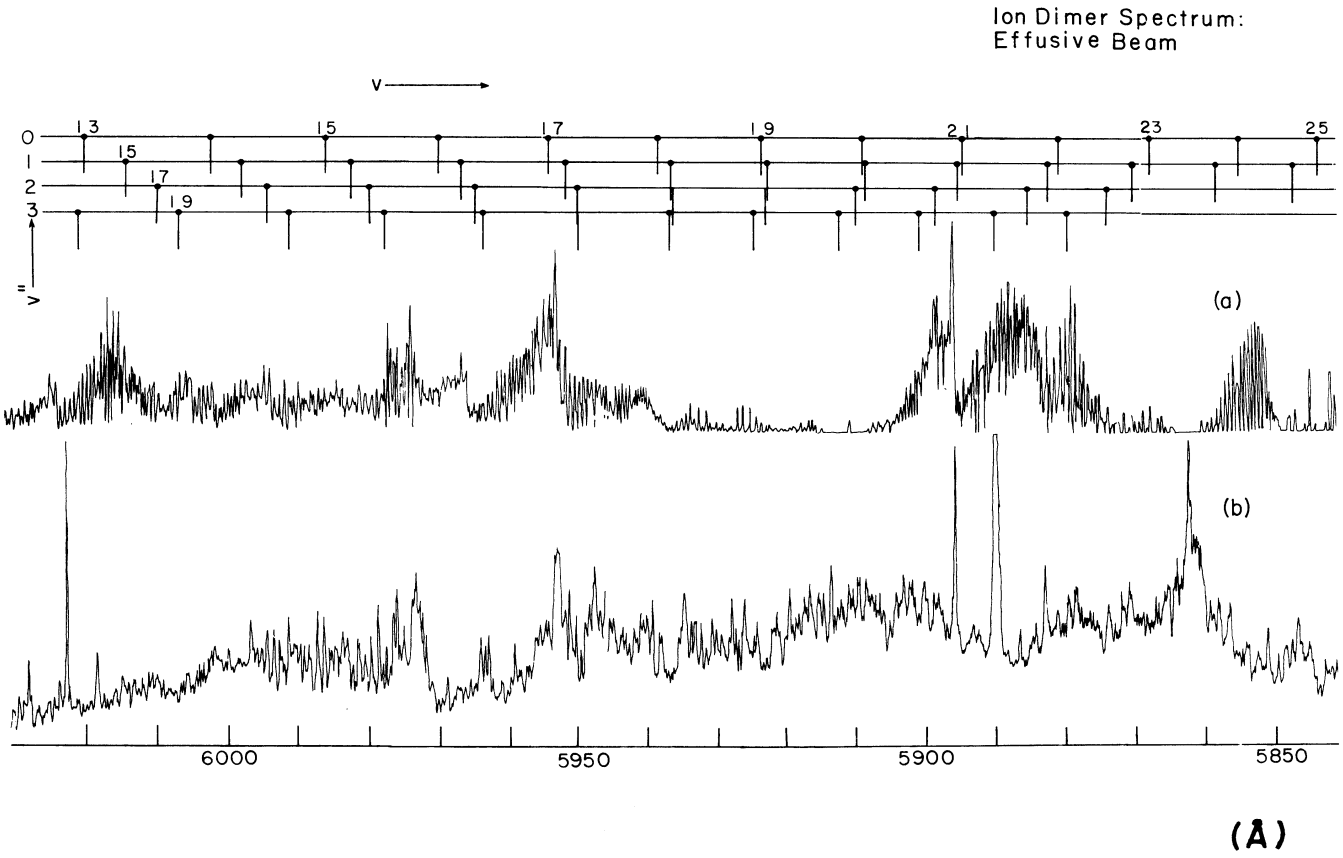

FIG. 4. (a) Model calculation of effusive-beam MPI spectrum of Na_2. (b) Observed ion dimer spectrum taken from Ref. 1.

$$N_2(t)=N_0(0)\frac{\sigma_2 I}{b}\left[1-\frac{b\exp(-at)-a\exp(-bt)}{b-a}\right], \quad (7)$$

where $a=\sigma_1 I^2$, $b=\sigma_2 I+\gamma$, and $N_1(0)$ is taken as the initial-state population derived from a Boltzmann distribution where the rotational and vibrational factors are obtained from different temperatures. The two temperatures arise from differing vibrational and rotational relaxation rates in the free-jet expansion.

We use Eq. (7) to generate calculated MPI spectra which includes the O, Q, and S branches (corresponding to $\Delta J=-2,0,+2$, respectively) for J'' up to 60 where we take

$$a=a'\omega^2\sum_i \frac{|\langle v'|v_i'\rangle|^2\,|\langle v_i'|v\rangle|^2}{\Delta\omega_i^2}. \quad (8)$$

In the model spectrum, each individual line is modulated by the calculated *rotationless* Franck-Condon factors (FCF), $|\langle v_i|v_j\rangle|^2$, and the intermediate state detuning $\Delta\omega_i$. The assumption here is that the FCF are weak functions of the rotational quantum number. The factor a', incorporating the electronic part of the transition probability $|d_{01}|^2|d_{12}|^2$ which we take to be constant, is given by

$$a'=\frac{8\pi}{2hc^2\Gamma}|d_{01}|^2|d_{12}|^2.$$

The values for a' and b in Eqs. (7) and (8) are fixed in any one calculated spectrum. We use these constants as variable parameters to obtain a calculated spectrum in Fig. 3(a) which best matches the cold beam result in Fig. 3(b). Without changing a' and b we then raise the model rotation-vibration temperatures and calculate a spectrum to compare with the effusive beam results. Figures 4(a) and 4(b) show the calculated and experimental effusive beam spectra along with the location of calculated band origins.

The molecular constants for the X state of Na_2 published by Kusch and Hessel,[11] the A state published by Kaminski,[12] and the $(3s+5s)^1\Sigma_g^+$ Rydberg level published by MXS were used to calculate the two-photon near-resonant transitions that couple the two levels together. We utilized the same spectral constants to generate Franck-Condon factors for the X-A and A-Rydberg rotationless transitions by using Gordon's method[13] on the Rydberg-Klein-Rees potential curves fit with cubic splines. We checked our results against the X-A FCF calculated by Zemke *et al.*[14] and found the agreement to be within 1%.

In the region between 6000 and 5880 Å we were able to match the general features of the cold spectrum quite well. The relative sizes of the $v\leftarrow v''$ (18,0) and $v\leftarrow v''$ (16,0) bands are correct and so are the shapes. Because of our ability to match the cold spectrum, this re-

gion provides a critical test of the contribution of the dimer mechanism to the effusive beam results. When we raise the model temperatures we reproduce some of the general features of the effusive beam spectrum reported in Ref. 3. Small shifts in band positions are due to the fact that higher, less well-determined vibrational levels of the excited state are observed. Note that in the region between 6000 and 5950 Å calculated and observed spectral features are generally in accord. At shorter wavelengths the match is poor. This may be due largely to inaccuracies in the molecular constants at the higher levels leading to incorrect band positioning and consequent inaccurate calculation of the Franck-Condon factors.

The model which we use to calculate the spectrum cannot reproduce every structural detail due to a number of limitations.

(1) The rate equation approach used here must be replaced by the optical Bloch equations when the rate of two-photon absorption is rapid compared to the rate of ionization.[15,16] Furthermore, we have ignored stimulated two-photon emission back to the initial state. These two effects are important when $\Delta\omega_i$ is small. Fortunately, the effects of these inaccuracies are diminished since, with small detuning and high laser intensity, signal saturation through depletion of initial-state molecules dominates. Hence the limiting effect on ion signal becomes initial-state population and not the photon absorption rate from the intermediate state.

(2) The model ignores any possible structure associated with the third photon which may arise from autoionizing states. Such structure has been observed by Martin *et al.* in sodium dimers.[17] By means of an optical-optical double resonance experiment, Martin *et al.* recorded transitions to high Rydberg states with vibrational levels above the ionization limit. However, in our experiment the three-photon absorption energy is above the dissociation limit of the Na_2^+ ground states, and, therefore, above the dissociation limit of any singly excited Rydberg level. These dissociative autoionizing states will not exhibit the sharp structure observed in our spectrum since they represent bound-free transitions in the nuclear as well as in the electronic wave functions, but they may broadly modulate the relative intensities of the vibrational bands. Furthermore, since the Rydberg state $(3s+5s)^1\Sigma_g^+$ and the Na_2^+ potential curves are similar, we expect that most of the Franck-Condon intensity will be concentrated in $\Delta v=0$ transitions. Therefore, the probability of transitions to these dissociative autoionizing states will be negligible.

(3) The model does not include potential-curve perturbations which may alter positions and intensities of the spectral lines in the two-photon absorption process. The large number of potential curves near the Rydberg levels increases the likelihood of perturbations. These perturbations may result in neutral Rydberg state predissociation (thereby decreasing ion dimer signal) or they may result in larger two-photon cross sections which would increase ion dimer signal.[18]

(4) The approximation made in going from Eq. (5) to Eq. (6) is valid for *intense O* and *S* branch lines since, due to selection rules, there will be only one nearby intermediate state. But in the case of the *Q* branch there will be two nearby intermediate states with rotational quantum numbers $J'=J''+1$ and $J'=J''-1$. If the photon energy falls between these intermediate states, the cross terms ignored in Eq. (6) will tend to cancel the diagonal terms due to sign changes in $\Delta\omega_i$ and the rate of two-photon absorption will be reduced. In fact, the terms may exactly cancel making the system transparent to two-photon absorption.[19,20] As the laser is scanned across an intense two-photon band the single-photon energy will move above, between, and then below the intermediate states—we discuss this point in a later section. The shape of the *Q* branch in the region where this takes place will be effected but the overall intensity of the band will not be greatly changed.

DISCUSSION

In conventional one-photon spectroscopy of diatomic molecules the relative intensity of a spectral line as a function of the rotational quantum number J depends on the Boltzmann factor, the degeneracy of the level, and the weak J dependence of the transition dipole moment given by the Hönl-London factors.[18] The classical spectroscopist knows *a priori* the general shape of a band even before he measures it. He is able to use this knowledge to make spectral assignments or to distinguish lines in the overlapping bands. In two-photon spectroscopy this situation is complicated by the detuning from resonance with the intermediate state. The problem was discussed by MXS, but because of its importance we emphasize the principle points in the context of this work. We plot in Fig. 5 *one-half* the energy of the rotational transitions of two-photon vibronic bands and the energy of a single-photon transi-

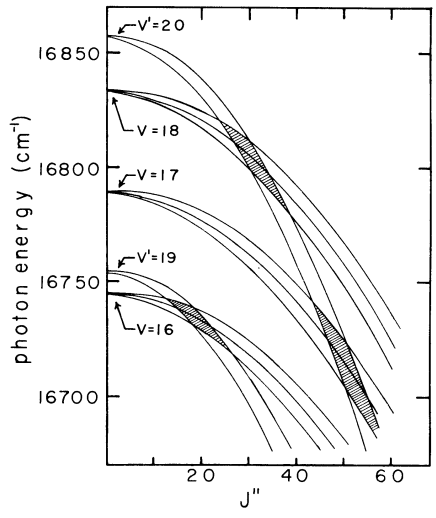

FIG. 5. Plots of one-half energy of the rotational progressions of two-photon vibronic bands v and the energy of single-photon transitions v', to the A state as a function of J''. Curves stemming from the same band origin represent different branches. The hatched areas indicate regions of expected spectral intensity maxima due to small intermediate state detuning, $\Delta\omega_i$.

tions to the A state as a function of J''. These curves are quadratics in J'' of the form

$$\nu=[\nu_0+BJ(J+1)-B''J''(J''+1)]/2 \tag{9a}$$

for the two-photon case and

$$\nu'=\nu_0'+B'J'(J'+1)-B''J''(J''+1) \tag{9b}$$

for the one-photon case, where the B's are the rotational constants for the states and ν_0 represents the origin of the band. Since the two-photon pathway involves states with ${}^1\Sigma_{g,u}^+$ symmetries (see Fig. 1), $\Delta J=\pm 1$ selection rules for each photon absorbed hold. Therefore, we need to consider only the O, Q, and S branches for the two-photon transition and the P and R branches for the one-photon intermediate. Also, the one-photon P branch is not coupled to the two-photon S branch nor the R branch to the O branch.

For a given J'', $\Delta\omega_i$ is the difference, $\nu'-\nu$, between the two-photon and one-photon curves in Fig. 5. The magnitude of $\Delta\omega_i^2$ is minimized for the value of J'' nearest to where the curves cross, and this minimum detuning point defines an intensity maximum in the rotational progression of a vibronic transition. Thus a qualitative understanding of the spectral intensity distribution can be gained by considering the relationships between the intermediate and Rydberg states which govern the positions of the curve crossings.

The point where the curves cross depends on the relative position of single- and two-photon band origins. We note that the curvatures of the lines formed by the two-photon transitions in Fig. 5 are about half that of the one-photon transitions. The reason is that for all branches the quadratic terms in Eq. (9) for the two-photon transition, $(B-B'')/2$, are approximately half that for the one-photon transition, $(B-B'')$. *In Na_2 these terms are negative and relatively large so that one-photon curves will not cross two-photon curves which start at higher energy.* In this case the intermediate state detuning diverges as J'' increases so that the one-photon intermediate state does not play a dominant role in determining the intensities in the rotational structure. For example, the closest real vibrational level of the A state to the $v\leftarrow v''$ (19,0) transition is only 18.4 cm^{-1} to the red at the origin; yet as we can see in the spectrum in Fig. 3(b) this band is barely discernable.

If the one-photon band origin is near and to the blue of a two-photon band origin then the curves will cross at small J''. In this case, we expect several intense lines since, when J'' is small, the lines are closely spaced and the rate of change of $\Delta\omega_i^2$ from one transition to the next is slow. In addition, at the band origin, the 3-GHz width of the laser will pump several transitions at once which increases the ion dimer signal. For cooled Na_2 the band is especially intense since the small-J'' rotational states are highly populated. An example from Fig. 5 is the $v'\leftarrow v''$ (19,0) band. The one-photon band origin is only 9.3 cm^{-1} to the blue of the two-photon Rydberg transition and, as shown in Fig. 3(b), the $v\leftarrow v''$ (16,0) transition is one of the more intense bands in the spectrum.

As a third example, Fig. 5 shows the $v'\leftarrow v''$ (20,0) intermediate transition is located 24.2 cm^{-1} to the blue of the $v\leftarrow v''$ (18,0) band origin. In this case the band origins are farther apart and the curves cross at high J''. The intensity of the observed band in Fig. 3(b) is not as strong as the $v\leftarrow v''$ (16,0) band because the individual rotational lines are farther apart, and $\Delta\omega_i^2$ is small only for a few transitions. We observe in the spectrum two maxima. The first is at the band origin and is due to the large population in the low-J'' states, a result of the cooled molecular beam. The position of the second maximum, as we expect, corresponds to the frequency where the curves in Fig. 5 cross. In Fig. 3(b) it appears that there is a third maximum to the red of the first two but this is due to the strong $v\leq v''$ (19,1) transition.

In a two-photon band, the value of J minimizing the detuning is not characterized by a simple rule since the energy of a one-photon transition is unrelated to the energy of a two-photon transition. Peak intensity positions of the spectrum cannot, in general, be matched to the calculated band origins. It is this lack of generality in the intensity envelope that makes analysis of MPI spectra difficult, particularly when the spectrum exhibits hot bands as it does in the effusive beam result.

In addition to the $(3s+5s)^1\Sigma_g^+$ state, we found only a few weak bands in our spectra due to the $(3s+4d)^1\Sigma_g^+$ state and no bands to the $(3s+4d)^1\Pi_g$ state.[21] An explanation of this is based on simple consideration of the Franck-Condon principle. The molecular constants for the Na_2 A state and the Rydberg states are similar. It follows that the shape of the potential curves are also similar. When this is the case, we expect that Franck-Condon factors are large when the difference in the vibrational quantum numbers, Δv, is small. Transitions to the intermediate A state from the $v''=0$ level range from $v'=18$ to 24. The two-photon transitions to the Rydberg levels range from 14 to 30 for the $(3s+5s)^1\Sigma_g^+$, from 5 to 12 for the $(3s+4d)^1\Sigma_g^+$, and from 0 to 7 for the $(3s+4d)^1\Pi_g$. Clearly Δv is small only for transitions to the $(3s+5s)^1\Sigma_g^+$ state in this spectral region. In fact we assign our largest peak to the $v\leftarrow v''$ (21,0) transition where the closest intermediate state is $v'=21$. To confirm this argument we calculate the Franck-Condon factors for the alternate Rydberg level transitions in this region and found them to be negligibly small.

Finally, we found that the $v\leftarrow v''$ (14,0) band is shifted over 3 Å to the blue of the calculated band origin. This is an intense peak which makes it an exception to our predictions since its band origin is to the blue of the nearest intermediate vibronic state. We speculate that this anomaly is due to perturbations in the potential curve. The level is probably perturbed by a bound state since if it were a dissociative state the line would be weaker not stronger.[18] Determination of the exact nature of these perturbations, however, is the proper subject of another study.

SUMMARY AND CONCLUSIONS

Our purpose in undertaking this study was to learn more about the mechanisms by which Na_2^+ is produced when sodium vapor is subjected to intense optical fields. While earlier studies have demonstrated that much of the dimer ion signal is due to laser-induced associative ioniza-

tion processes, our ignorance of the detailed MPI mechanism in Na_2 prevented us from gauging the significance of this process. Through the use of an intense, cooled molecular beam produced by free-jet expansion of sodium vapor, we obtained a greatly simplified MPI spectrum. Modeling of the MPI process allowed us to calculate spectra which match many of the features of the cold-beam experimental result and some of the features of the effusive-beam spectrum in a limited spectral region. However, neither our rate equation model nor the Na_2 excited-state spectral constants are sufficiently refined to permit a match to every one of the multitudinous number of peaks appearing in the effusive-beam spectrum.

Even if a theoretical match to every peak is too much to ask, one may legitimately question why the experimental sharp features (presumed to arise from two-photon resonant, three-photon MPI) do not match the two-photon resonances reported by MXS. The answer may be in the vastly different optical power densities of the two experiments. The MPI process was generated by megawatt laser pulses, and a simple calculation shows that these are sufficient to produce ac Stark shifts in the $(3s+5s)^1\Sigma_g^+$ Rydberg state ranging from 0.5 to 5 cm^{-1}. Shifts of this magnitude could distort the spectrum sufficiently to produce a mismatch between the two sets of results. Closer scrutiny of this possibility is however beyond the scope of the present study.

From the earlier work of Boulmer and Weiner[3] and from the present study it is apparent that both laser-induced collisions and MPI are important contributions to ion dimer production. The finer structure of the spectra, which appears to be due to MPI, rides on a broad envelope of signal arising from laser-induced associative ionization.

ACKNOWLEDGMENTS

The authors thank Paul Julienne and Millard Alexander for the use of their computer codes. This work was supported by the NSF Grant No. Phy-83-05086. Computer time for this project was supported through the facilities of the Computer Science Center of the University of Maryland.

[1]P. Polak-Dingels, J.-F. Delpech, and J. Weiner, Phys. Rev. Lett. **44**, 1663 (1980).

[2]F. Roussel, B. Carré, P. Breger, and G. Spiess, J. Phys. B **14**, L313 (1981).

[3]J. Boulmer and J. Weiner, Phys. Rev. A **27**, 2817 (1983).

[4]C. Y. R. Wu (private communication).

[5]G. P. Morgan, H.-R. Xia, and A. L. Schawlow, J. Opt. Soc. Am. **72**, 315 (1982).

[6]D. L. Feldman, Ph. D. Thesis, Columbia University, University Microfilm International, Ann Arbor, Michigan, 1978 (unpublished).

[7]W. C. Wiley and I. H. McLaren, Rev. Sci. Instrum. **26**, 1150 (1955).

[8]R. D. Hudson, Phys. Rev. **135**, A1212 (1964).

[9]P. Cremaschi, P. M. Johnson, and J. L. Whitten, J. Chem. Phys. **69**, 4341 (1978).

[10]D. H. Parker, J. O. Berg, and M. A. El-Sayed, in *Advances in Laser Chemistry*, edited by B. H. Zewail (Springer, Berlin, 1978).

[11]P. Kusch and M. M. Hessel, J. Chem. Phys. **68**, 2591 (1978).

[12]M. E. Kaminski, J. Chem. Phys. **66**, 4951 (1977); **73**, 3520(E) (1980).

[13]R. G. Gordon, J. Chem. Phys. **51**, 14 (1969).

[14]W. T. Zemke, K. K. Verma, T. Vu, and W. C. Stwalley, J. Mol. Spectrosc. **85**, 150 (1981).

[15]J. R. Ackerhalt and J. H. Eberly, Phys. Rev. A **14**, 1705 (1976).

[16]B. W. Shore and J. Ackerhalt, Phys. Rev. A **15**, 1640 (1977).

[17]S. Martin, J. Chevaleyre, S. Valignat, J. F. Perrot, M. Broyer, B. Cabaud, and A. Hoareau, Chem. Phys. Lett. **87**, 235 (1982).

[18]G. Herzberg, *Molecular Spectra and Molecular Structure*, 2nd ed. (Van Nostrand, Princeton, 1950).

[19]J. E. Bjorkholm and P. J. Liao, Phys. Rev. Lett. **33**, 128 (1974).

[20]A. Quattropani, F. Bassani, and S. Carillo, Phys. Rev. A **25**, 3079 (1982).

[21]N. W. Carlson, A. J. Taylor, K. M. Jones, and A. L. Schawlow, Phys. Rev. A **24**, 822 (1981).